

Cite this: *Nanoscale Adv.*, 2019, 1, 189

# Photocatalytic overall water splitting on Pt nanocluster-intercalated, restacked $\text{KCa}_2\text{Nb}_3\text{O}_{10}$ nanosheets: the promotional effect of co-existing ions†

Takayoshi Oshima,<sup>ab</sup> Yunan Wang,<sup>c</sup> Daling Lu,<sup>d</sup> Toshiyuki Yokoi<sup>c</sup>  
and Kazuhiko Maeda<sup>ib</sup>\*<sup>a</sup>

Promotional effects of co-existing ions on overall water splitting into  $\text{H}_2$  and  $\text{O}_2$  have been studied in bulk-type semiconductor photocatalysts (e.g.,  $\text{TiO}_2$ ), but such an effect remains unexplored in two-dimensional nanosheet photocatalysts. Here we examined the effect of co-existing ions on the photocatalytic water splitting activity of Pt nanocluster-intercalated  $\text{KCa}_2\text{Nb}_3\text{O}_{10}$  nanosheets. Interestingly, not only anions, as usually observed in bulk-type photocatalysts, but also cations had a significant influence on the photocatalytic performance. The rates of  $\text{H}_2$  and  $\text{O}_2$  evolution over  $\text{Pt/KCa}_2\text{Nb}_3\text{O}_{10}$  as well as the product stoichiometry were improved in the presence of  $\text{NaI}$ .  $\text{I}^-$  ions were found to effectively suppress undesirable backward reactions, consistent with the previous work by Abe *et al.* (*Chem. Phys. Lett.*, 2003, 371, 360–364). On the other hand,  $\text{Na}^+$  ions in the reaction solution were exchanged for  $\text{K}^+$  in the interlayer space of  $\text{KCa}_2\text{Nb}_3\text{O}_{10}$  during the water splitting reaction, which promoted interlayer hydration and consequently improved photocatalytic performance.

Received 25th September 2018  
Accepted 3rd December 2018

DOI: 10.1039/c8na00240a

rsc.li/nanoscale-advances

## Introduction

Clean production of hydrogen by water splitting over a semiconductor photocatalyst has attracted considerable interest in order to meet the social demand for replacing  $\text{CO}_2$ -emitting fossil fuels with clean energy sources.<sup>1–3</sup> The efficiency of photocatalytic water splitting, however, still remains unsatisfactory. Therefore, not only enhancing the performance of known photocatalysts but also fundamental investigation, for example understanding the reaction mechanism and exploring new materials, is important in this research field.

Certain layered materials undergo exfoliation, producing colloidal suspensions of unilamellar sheets.<sup>4–27</sup> The planar size of the exfoliated sheets typically ranges from several hundreds of nanometers to a few micrometers, with a thickness of 1–2 nm. Because of the sheet-like two-dimensional (2D) structure, it is

called a nanosheet. The nanosheets containing certain transition metal cations such as  $\text{Ti}^{4+}$ ,  $\text{Nb}^{5+}$ ,  $\text{Ta}^{5+}$ , and  $\text{W}^{6+}$  are known to exhibit photocatalytic activity. They are expected to have several advantages in heterogeneous photocatalysis, compared with conventional bulk-type 3D photocatalysts (e.g.,  $\text{TiO}_2$ ).

It is known that high crystallinity of a semiconductor has a positive impact on photocatalytic performance for overall water splitting, because of the prolonged lifetime of photo-generated electrons and holes.<sup>28</sup> To obtain a highly crystalline material, high calcination temperature is generally required in the synthesis process; however, such harsh calcination conditions facilitate grain growth of photocatalyst particles, resulting in smaller surface area and lower density of reaction sites, and *vice versa*.<sup>29</sup> Moreover, larger size of semiconductor particles can have a negative effect in terms of carrier diffusion to the surface, resulting in recombination between electrons and holes and lowering photocatalytic activity. On the other hand, a nanosheet has both high crystallinity and high surface area owing to its single-crystalline character and anisotropic structure.<sup>30</sup> Furthermore, the small thickness of the nanosheet is expected to shorten the migration distance of photogenerated carriers to the surface, thereby reducing the recombination probability.<sup>9,12</sup> Despite these fascinating features, there are a limited number of examples of overall water splitting using a nanosheet photocatalyst.

Other than such structural factors, there are some key factors to achieve high photocatalytic performance. One of them is

<sup>a</sup>Department of Chemistry, School of Science, Tokyo Institute of Technology, 2-12-1-NE-2, Ookayama, Meguro-ku, Tokyo 152-8550, Japan. E-mail: maedak@chem.titech.ac.jp

<sup>b</sup>Japan Society for the Promotion of Science, Kojimachi Business Center Building, 5-3-1, Kojimachi, Chiyoda-ku, Tokyo 102-0083, Japan

<sup>c</sup>Nanospace Catalysis Unit, Institute of Innovative Research, Tokyo Institute of Technology, 4259-S2-5, Nagatsuta, Midori-ku, Yokohama 226-8503, Japan

<sup>d</sup>Center for Advanced Materials Analysis, Tokyo Institute of Technology, 4259-R1-34, Nagatsuta-cho, Midori-ku, Yokohama 226-850, Japan

† Electronic supplementary information (ESI) available. See DOI: 10.1039/c8na00240a







and O<sub>2</sub> was introduced in a closed reaction system and the amount was monitored under dark conditions, as shown in Fig. 3. Although the backward reaction over bare KCa<sub>2</sub>Nb<sub>3</sub>O<sub>10</sub> was negligible in pure water, a decrease of H<sub>2</sub> and O<sub>2</sub> was observed over Pt/KCa<sub>2</sub>Nb<sub>3</sub>O<sub>10</sub>, indicating that the backward reaction took place on Pt. The water formation rate over Pt/KCa<sub>2</sub>Nb<sub>3</sub>O<sub>10</sub> became slower in the presence of NaI than in pure H<sub>2</sub>O. On the other hand, the backward reaction rate in aqueous Na<sub>2</sub>SO<sub>4</sub> solution was almost the same as that in pure water. These results suggest that the I<sup>-</sup>, not Na<sup>+</sup>, interacted with Pt and suppressed the backward reactions, which are most likely to occur on the externally deposited Pt, contributing to higher photocatalytic activity. Note here that SO<sub>4</sub><sup>2-</sup> is in principle unreactive during the photocatalytic reaction.<sup>35</sup>

We attempted to detect the iodine species adsorbed on Pt/KCa<sub>2</sub>Nb<sub>3</sub>O<sub>10</sub> after the water splitting reaction. However, no iodine signal was observed in this sample (Fig. S2†), most likely because I<sup>-</sup> cannot interact with the intercalated Pt due to electrostatic repulsion between negatively charged nanosheets and I<sup>-</sup>. On the other hand, a small, but distinct photoelectron signal attributable to I 3d was detected in the restacked KCa<sub>2</sub>Nb<sub>3</sub>O<sub>10</sub> nanosheets that consisted of externally deposited Pt nanoparticles. It in turn indicates that the number of externally deposited Pt nanoparticles in the present Pt/KCa<sub>2</sub>Nb<sub>3</sub>O<sub>10</sub> was not large enough to produce an observable quantity of iodine layers by XPS. Nevertheless, backward reactions that occurred on such lower density Pt islands are significant, and the suppression of the backward reactions is essential. In the photocatalytic reaction, I<sup>-</sup> also improved the H<sub>2</sub>/O<sub>2</sub> stoichiometry. It is known that photo-reduction of O<sub>2</sub> proceeds very efficiently on Pt nanoparticles, reducing the O<sub>2</sub> evolution performance.<sup>38</sup> Therefore, the improved stoichiometry would originate from the suppression of O<sub>2</sub> photo-reduction on Pt as well.

I<sup>-</sup> is often used as an electron mediator between H<sub>2</sub> and O<sub>2</sub> evolution photocatalysts in Z-scheme water splitting.<sup>33,38–41</sup> One may suspect that I<sup>-</sup> has a negative impact on photocatalytic

performance because the oxidation of I<sup>-</sup> on the semiconductor surface hinders water oxidation, which has been observed in Pt/TiO<sub>2</sub> at high concentration of NaI.<sup>32</sup> Thus, we investigated the dependence of water splitting performance of Pt/KCa<sub>2</sub>Nb<sub>3</sub>O<sub>10</sub> on the NaI concentration. Fig. 4 displays a relationship between H<sub>2</sub>/O<sub>2</sub> evolution rates in the water splitting reaction and NaI concentration. H<sub>2</sub> and O<sub>2</sub> evolution rates monotonically increased up to 10 mM NaI and reached a plateau at higher concentration of NaI. UV-visible absorption spectroscopy indicated that before and after the photocatalytic reaction in 10 mM NaI solution, the concentration of I<sup>-</sup> remained almost unchanged. These facts indicate that the oxidation of H<sub>2</sub>O, not I<sup>-</sup>, dominated on KCa<sub>2</sub>Nb<sub>3</sub>O<sub>10</sub>. Adsorption isotherm measurement of NaI revealed that no adsorption of I<sup>-</sup> took place on the surface of bare KCa<sub>2</sub>Nb<sub>3</sub>O<sub>10</sub>. The surface properties inhibited the oxidation of I<sup>-</sup> on KCa<sub>2</sub>Nb<sub>3</sub>O<sub>10</sub>, leading to O<sub>2</sub> evolution even in the presence of higher concentration of NaI.

### Effect of Na<sup>+</sup>

As demonstrated above, the photocatalytic activity of Pt/KCa<sub>2</sub>Nb<sub>3</sub>O<sub>10</sub> restacked nanosheets for overall water splitting was promoted in the presence of Na<sup>+</sup> as well. In order to elucidate the reason, the reacted Pt/KCa<sub>2</sub>Nb<sub>3</sub>O<sub>10</sub> samples in the presence of various salts were characterized by XRD. Fig. 5 displays the X-ray diffraction peaks of Pt/KCa<sub>2</sub>Nb<sub>3</sub>O<sub>10</sub> attributed to the (002) plane, which is the stacking direction of restacked nanosheets. The diffraction peaks were shifted to lower two-theta directions after photocatalytic reactions in all cases, indicating that the (002) plane distance, namely the interlayer distance of restacked nanosheets, was expanded most likely due to an intercalation of water in the interlayer space, as reported previously.<sup>6</sup> It should be noted that the peak positions were altered depending on the cations in the reaction solution. Pt/KCa<sub>2</sub>Nb<sub>3</sub>O<sub>10</sub> after photocatalytic reaction in the presence of Na<sup>+</sup> exhibited 002 diffraction peaks at lower two-theta positions compared to the peaks

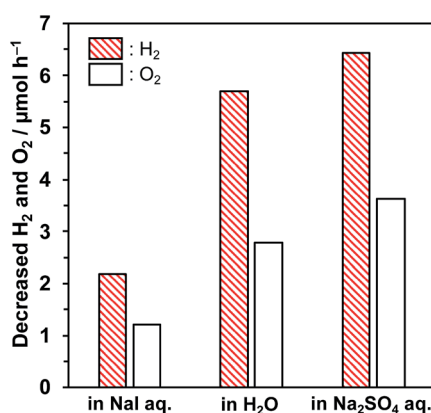


Fig. 3 Decreasing rates of H<sub>2</sub> and O<sub>2</sub> evolution over Pt/KCa<sub>2</sub>Nb<sub>3</sub>O<sub>10</sub> in aqueous NaI solution (10 mM), pure water, and Na<sub>2</sub>SO<sub>4</sub> solution (5 mM) under dark conditions. Reaction conditions: photocatalyst, 50 mg; reactant volume, 100 mL; introduced amount of H<sub>2</sub>, ca. 200 μmol and O<sub>2</sub>, ca. 100 μmol.

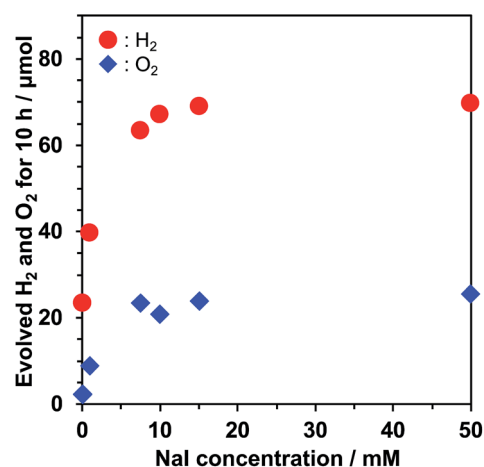


Fig. 4 Dependence of the photocatalytic water splitting activity of Pt/KCa<sub>2</sub>Nb<sub>3</sub>O<sub>10</sub> on the NaI concentration. Reaction conditions: catalyst, 50 mg; reaction solution, 100 mL; light source, a 300 W Xe lamp (λ ≥ 300 nm).







## Conflicts of interest

There are no conflicts to declare.

## Acknowledgements

This work was partially supported by a Grant-in-Aid for Scientific Research on Innovative Areas "Mixed Anion" (Project JP16H06441) from the Japan Society for the Promotion of Science (JSPS). T. O. wishes to acknowledge support by a JSPS Fellowship for Young Scientists (Project JP16J10084). The authors thank Prof. Masashi Hattori and Michikazu Hara (Tokyo Institute of Technology) for assistance in XPS measurements.

## Notes and references

- 1 A. Kudo and Y. Miseki, *Chem. Soc. Rev.*, 2009, **38**, 253–278.
- 2 K. Maeda, *J. Photochem. Photobiol., C*, 2011, **12**, 237–268.
- 3 Y. Wang, H. Suzuki, J. Xie, O. Tomita, D. J. Martin, M. Higashi, D. Kong, R. Abe and J. Tang, *Chem. Rev.*, 2018, **118**, 5201–5241.
- 4 R. E. Schaak and T. E. Mallouk, *Chem. Mater.*, 2000, **12**, 2513–2516.
- 5 Y. Ebina, T. Sasaki, M. Haruda and M. Watanabe, *Chem. Mater.*, 2002, **14**, 4390–4395.
- 6 Y. Ebina, N. Sakai and T. Sasaki, *J. Phys. Chem. B*, 2005, **109**, 17212–17216.
- 7 H. Hata, S. Kudo, Y. Kobayashi and T. E. Mallouk, *J. Am. Chem. Soc.*, 2007, **129**, 3064–3065.
- 8 S. Ida, C. Ogata, K. Izawa, T. Inoue, O. Altuntasoglu and Y. Matsumoto, *J. Am. Chem. Soc.*, 2007, **129**, 8956–8957.
- 9 H. Hata, Y. Kobayashi, V. Bojan, W. J. Youngblood and T. E. Mallouk, *Nano Lett.*, 2008, **8**, 794–799.
- 10 S. Ida, C. Ogata, M. Eguchi, W. J. Youngblood, T. E. Mallouk and Y. Matsumoto, *J. Am. Chem. Soc.*, 2008, **130**, 7052–7059.
- 11 R. Ma, Y. Kobayashi, W. J. Youngblood and T. E. Mallouk, *J. Mater. Chem.*, 2008, **18**, 5982–5985.
- 12 K. Maeda, M. Eguchi, W. J. Youngblood and T. E. Mallouk, *Chem. Mater.*, 2008, **20**, 6770–6778.
- 13 M. C. Sarahan, E. C. Carroll, M. Allen, D. S. Larsen, N. D. Browning and F. E. Osterloh, *J. Solid State Chem.*, 2008, **181**, 1678–1683.
- 14 K. Maeda, M. Eguchi, W. J. Youngblood and T. E. Mallouk, *Chem. Mater.*, 2009, **21**, 3611–3617.
- 15 K. Maeda and T. E. Mallouk, *J. Mater. Chem.*, 2009, **19**, 4813–4818.
- 16 M. R. Allen, A. Thibert, E. M. Sabio, N. D. Browning, D. S. Larsen and F. E. Osterloh, *Chem. Mater.*, 2010, **22**, 1220–1228.
- 17 E. M. Sabio, M. Chi, N. D. Browning and F. E. Osterloh, *Langmuir*, 2010, **26**, 7254–7261.
- 18 S. Ida and T. Ishihara, *J. Phys. Chem. Lett.*, 2014, **5**, 2533–2542.
- 19 S. Ida, A. Takashiba, S. Koga, H. Hagiwara and T. Ishihara, *J. Am. Chem. Soc.*, 2014, **136**, 1872–1878.
- 20 K. Maeda, M. Eguchi and T. Oshima, *Angew. Chem., Int. Ed.*, 2014, **53**, 13164–13168.
- 21 T. Oshima, O. Ishitani and K. Maeda, *Adv. Mater. Interfaces*, 2014, **1**, 1400131.
- 22 K. Maeda, G. Sahara, M. Eguchi and O. Ishitani, *ACS Catal.*, 2015, **5**, 1700–1707.
- 23 T. Oshima, D. Lu, O. Ishitani and K. Maeda, *Angew. Chem., Int. Ed.*, 2015, **54**, 2698–2702.
- 24 T. Oshima, M. Eguchi and K. Maeda, *ChemSusChem*, 2016, **9**, 396–402.
- 25 T. Oshima, D. Lu and K. Maeda, *ChemNanoMat*, 2016, **2**, 748–755.
- 26 Y. Xia, W. Chen, S. Liang, J. Bi, L. Wu and X. Wang, *Catal. Sci. Technol.*, 2017, **7**, 5662–5669.
- 27 Y. Xia, S. Liang, L. Wu and X. Wang, *Catal. Today*, 2018, DOI: 10.1016/j.cattod.2018.03.061.
- 28 F. Amano, A. Yamakata, K. Nogami, M. Osawa and B. Ohtani, *J. Am. Chem. Soc.*, 2008, **130**, 17650–17651.
- 29 A. Kudo, A. Tanaka, K. Domen and T. Onishi, *J. Catal.*, 1988, **111**, 296–301.
- 30 K. Maeda and T. E. Mallouk, *Bull. Chem. Soc. Jpn.*, 2018, DOI: 10.1246/bcsj.20180258.
- 31 K. Sayama and H. Arakawa, *J. Chem. Soc., Faraday Trans.*, 1997, **93**, 1647–1654.
- 32 R. Abe, K. Sayama and H. Arakawa, *Chem. Phys. Lett.*, 2003, **371**, 360–364.
- 33 R. Abe, K. Sayama and H. Sugihara, *J. Phys. Chem. B*, 2005, **109**, 16052–16061.
- 34 H. Kato, Y. Sasaki, A. Iwase and A. Kudo, *Bull. Chem. Soc. Jpn.*, 2007, **80**, 2457–2464.
- 35 K. Maeda, H. Masuda and K. Domen, *Catal. Today*, 2009, **147**, 173–178.
- 36 Y. Miseki, H. Kusama, H. Sugihara and K. Sayama, *Chem. Lett.*, 2010, **39**, 846–847.
- 37 H. Suzuki, O. Tomita, M. Higashi and R. Abe, *J. Mater. Chem. A*, 2017, **5**, 10280–10288.
- 38 R. Abe, M. Higashi and K. Domen, *ChemSusChem*, 2011, **4**, 228–237.
- 39 M. Higashi, R. Abe, K. Teramura, T. Takata, B. Ohtani and K. Domen, *Chem. Phys. Lett.*, 2008, **452**, 120–123.
- 40 K. Maeda, M. Higashi, D. Lu, R. Abe and K. Domen, *J. Am. Chem. Soc.*, 2010, **132**, 5858–5868.
- 41 K. Maeda, D. Lu and K. Domen, *ACS Catal.*, 2013, **3**, 1026–1033.
- 42 M. Machida, T. Mitsuyama, K. Ikeue, S. Matsushima and M. Arai, *J. Phys. Chem. B*, 2005, **109**, 7801–7806.
- 43 T. Oshima, T. Yokoi, M. Eguchi and K. Maeda, *Dalton Trans.*, 2017, **46**, 10594–10601.

